한국동력기계공학회지 제17권 제5호 pp. 13-22 2013년 10월 (ISSN 1226-7813)
Journal of the Korean Society for Power System Engineering, Vol. 17, No. 5, pp. 13-22, October 2013
Research paper

Physicochemical Characteristics Based on Hydrothermal Aging of Prepared DOC

Choong-Kil Seo*†

(received 31 July 2013, revised 09 October, accepted 09 October 2013)

Abstract : This paper reports the investigation of the physical and chemical characteristics of the prepared 3Pt-2MgO-3ZrO_2-2CeO_2/Al_2O_3 DOC, based on its hydrothermal aging. As a result of impregnating and reducing the $H_2PtCl_6 \cdot 6H_2O$ precursor on a γ-Al_2O_3 basis, it was well dispersed into small particles with the range 2-3nm. This was because the Al_2O_3 acted as a barrier to prevent movement of the catalyst particles. For a hydrothermally aged catalyst for 9h at 700℃, its performance when purifying harmful gases decreased compared to a fresh catalyst, but its specific surface area was at the same level. This was because the performance of the catalyst was reduced by the sintering of the precious metal Pt, rather than by washcoat sintering and pore clogging. For an excessively hydrothermally aged catalyst for 9h at 850℃, Pt grew into an approximately 50nm class, formed a cluster compared to a fresh catalyst. The CeO_2 promoters also formed clusters among components of the same type, reducing their specific surface area to 114m^2/g, which was 14% less than a fresh catalyst.

Key Words : Diesel Engine, DOC (Diesel Oxidation Catalyst), Hydrothermal Aging, Pt, Promoter

1. Introduction

Diesel engines are increasing in market demand in general passenger cars as well as commercial vehicles due to strong power, high fuel economy and efficiency, and low CO_2 emissions. The harmful exhaust gases generated during the operation of a diesel engine include CO, NOx, HC, and particulate material (PM). The after-treatment devices to reduce the amount of exhaust gases include diesel oxidation catalyst (DOC), de-NOx (LNT, SCR) catalyst, and DPF. Among these, DOC reduces the exhaust gases by oxidizing CO, HC and NOx, and activating NOx catalytic reduction and DPF mounted to its downstream[1~2]. The recent times have seen an increase in the importance of after-treatment devices in order to meet the strict Euro 6 emission standards. Therefore, Given this trend, it is important to develop a high-speed aging mode to shorten the period of developing after-treatment devices. Recently, studies on the performance and durability of DOC catalysts mounted as a basic system for the after-treatment of diesel automobiles have been partially carried out[3~12]. However, in the previous studies, it was not easy to clearly analyze the mechanism based on the hydrothermal aging of commercial DOC composed of various catalyst materials.

*† Choong-Kil Seo (corresponding author) : Department of Automotive & Mechanical Engineering, Howon University.
E-mail : ckseo@howon.ac.kr, Tel : 063-450-7215

This study manufactured 3Pt-2MgO-3ZrO_2-2CeO_2/Al_2O_3 DOC, a basic component making up a commercial DOC. The purpose of this study is to analyze the fundamental physical and chemical characteristics based on the hydrothermal aging to determine the conditions responsible for the highest deactivation of the catalyst.

2. Experimental setup and method

2.1 Catalyst preparation and characterization

The 3Pt-2MgO-3ZrO_2-2CeO_2/Al_2O_3 DOC was prepared by the conventional impregnation method. First, 0.557g of $H_2PtCl_6 \cdot 6H_2O$ placed in 50mL of distilled water at 80℃ and stirred for 6h. The solution was dried in an oven at 80℃ for 24h, and the catalyst powder was calcinated in air at 2 L/min for 5 h at 500℃. Using the same method, MgO (0.14g), ZrO_2 (0.21g) and CeO_2 (0.14g) additive catalysts were placed in 50mL of distilled water at 80℃ and stirred for 6h. Afterward, the drying and calcination process was repeated. A cordierite substrate was coated by dipping it in 3Pt-2MgO-3ZrO_2-2CeO_2/Al_2O_3 in aqueous suspension. The slurry was stirred for 2h. Each monolith was dipped 2–3times. After each dip, the excess slurry was carefully removed by blowing air through the channels and the catalyst was dried at 200℃ for 2 h and then weighed. When the washcoat loading was approximately 70 g/L, the catalyst was calcinated in air at 2 L/min for 5h at 500℃. The size and size distribution of Pt and additive catalyst particles on the catalyst surface were observed using transmission electron microscopy (TEM, JEM-2000FXII (200kV), JEOL) equipped with an energy-dispersive X-ray (EDX) detector. The surface cells on the catalyst were observed using scanning electron microscopy (SEM; JSM-7500F + EDS (Oxford)). The Brunauer–Emmett–Teller (BET) method was used to measure the specific surface areas, pore volumes and pore size distributions of the catalyst samples (ASAP 2020, Micromeritics). Before the measurements, all of the samples were degassed to 1×10^{-4} torr. The adsorption isotherms were obtained after degassing the pre-adsorbed hydrogen at 300℃ and 1×10^{-6} torr for 0.5h. The crystalline structure of the catalysts based on the hydrothermal aging conditions was measured using a multi-purpose X-ray diffraction (XRD, X'Pert PRO, PANalytical) device[13].

2.2 Experimental apparatus and conditions

The catalytic reaction apparatus is comprised of a gas supply part, catalytic reaction part, an analyzer, and controllers.

Table 1 shows the composition of model gas components, determined by considering the gases emitted from a diesel engine. The overall flow rate of the model gases was set to 18L/min (space velocity 25,000 h^{-1}) as a basis.

Table 1 Model gas components for evaluating DOC

Gas components	Composition
NO (ppm)	500
CO (ppm)	500
THC(ppmC_1)	500
O_2(%)	13
CO_2(%)	7
N_2	Balance
SV(h^{-1})	25,000

The temperature of the DOC catalysts was controlled by using the temperature controller in the electric furnace. The manufactured DOCs were inserted into the center of a reaction tube in with dimensions 30×30×50mm (W×D×H). To evaluate the performance of the DOC, the temperature was raised to 100~375℃ at 4℃/min, and, after the

catalytic reaction, the gas components were quantitatively and qualitatively analyzed every second by using an MRU analyzer (VARIO plus Industrial, MRU Instruments, Inc.) by an IR and electrochemical cell analysis method. H_2O can reduce the analysis ability of an MRU analyzer, if it enters the analyzer during the catalytic reaction. Thus, H_2O was not simulated during the catalytic reaction.

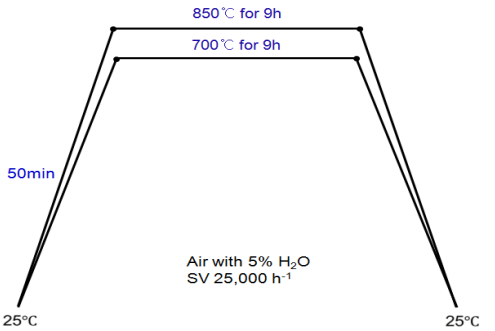

Fig. 1 Mode of hydrothermal aging

Fig. 1 shows the mode of hydrothermal aging. The hydrothermal aging was conducted on the DOC catalyst by supplying air (2L/min) through a humidifier with 5% saturated vapor pressure into an electric furnace at either 750℃ or 900℃.

2.3 Evaluation of performance

The DOC conversion ratio was investigated at catalyst temperatures in the range 100~375℃ in transient mode at a heating rate of 4℃/min. The conversion ratio was calculated using Eq. (1).

$$Conversion(\%) = \frac{(Gases_{inlet} - Gases_{outlet})}{Gases_{inlet}} \times 100(\%) \quad (1)$$

In Eq. (1), $Gases_{in}$ and $Gases_{out}$ are the gas concentrations at the inlet and outlet of the catalyst, respectively. The model gas used for evaluating the DOC catalysts comprised 500ppm NO, 500ppm CO, 500ppmC_1 THC, 13% O_2, and 7% CO_2 in a N_2 balance (SV 25,000 h^{-1}).

3. Experimental results and discussion

3.1 Basic characteristics of catalyst components

For the physical and chemical analysis of DOCs based on the hydrothermal aging, it is important to understand the basic characteristics of Pt and promoters.

Figs. 2 and 3 show the TEM/SEM photographs of the catalysts and promoters. Figs. 2 (a) and 3 (a) show the photographs of Pt acting as a major oxidizer in the DOC.

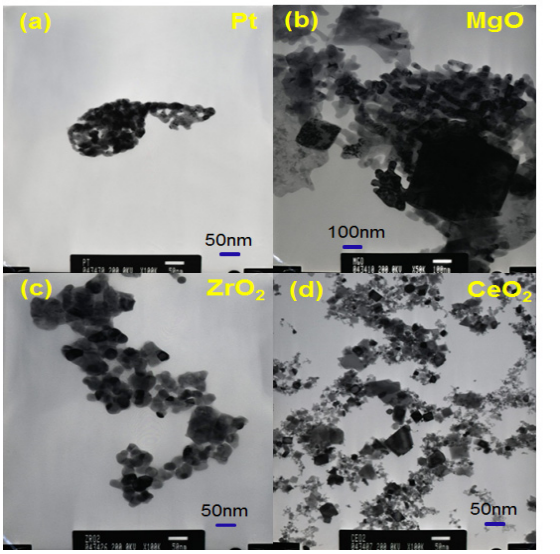

Fig. 2 TEM photographs of Pt and promoters

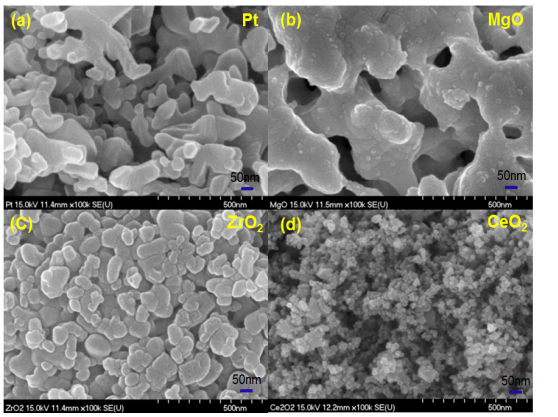

Fig. 3 SEM photographs of Pt and promoters

In order to extract Pt, the $H_2PtCl_6 \cdot 6H_2O$ precursor (powder) was first precipitated in a liquid phase, and then its aqueous solution was collected in a combustion board in the reaction tube. After evaporating the solution by supplying 2L/min of air for 30 min at 300℃, the precusor was reduced with 1% H_2. In the case of fresh device, the Pt loaded in an after-treatment device is typically loaded on a support in a 2~3nm sized support[14]. However, the Pt in Figs. 2 (a) and 3 (a) show an irregular shape, with particles agglomerated in the range 20~50nm. This is because when Pt particles were not loaded on a support, they migrated and agglomerated among components of the same type. Figs. 2 (b) and 3 (b) show the photographs of MgO. MgO was loaded to increase the pores, which can improve the performance of catalysts by increasing their reaction sites. Large particles of size ≥ 50nm are agglomerated. Figs. 2 (c) and 3 (c) show that ZrO_2 making formed a monoclinic crystal with a size of 30~50nm. ZrO_2 is a stabilizer with a high melting point (2720℃) that reduces washcoat sintering, acting as adjusting acid sites in a SCR catalyst[13].

Figs. 2 (d) and 3 (d) show that CeO_2 reduced the thermal sintering of the catalysts and supported their activity. It had a fluorite crystal structure with a size of approximately 20~40nm, also act in gas an oxygen storage capacity (OSC). This OSC discharges oxygen necessary for a change in valence from Ce^{4+} to Ce^{3+}in cerium in are reduction atmosphere and stores and restores excess oxygen in gas into and from a crystal in an oxidation atmosphere.

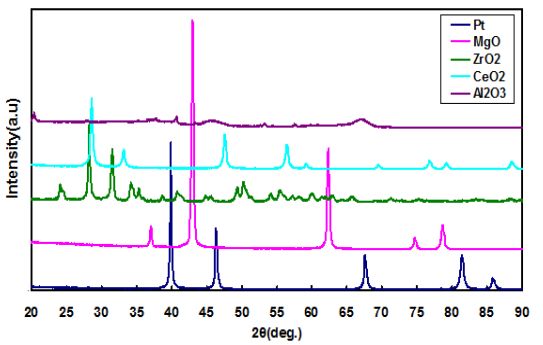

Fig. 4 XRD spectra of Pt and promoters

Fig. 4 shows the XRD peaks of Pt and promoters. Pt controls the conversion performance of harmful gases in DOC. As shown in Figs. 2 (a) and 3 (a), only Pt was extracted from the $H_2PtCl_6 \cdot 6H_2O$ precursor (powder). Because the main peak of Pt is 2θ=39.7°, as seen in Fig. 4, Pt was not oxidized after being extracted from the precursor, but existed only as Pt. In addition, it is known that, for 2θ=35.09°, Pt (Ⅱ) oxide and/or Pt (Ⅳ) oxide exist[15~16].

3.2 Manufacturing process for DOC

Based on the fundamental characteristics of the precursor for a DOC, this study studied the manufacturing process for DOC ($3Pt\text{-}2MgO\text{-}3ZrO_2\text{-}2CeO_2/Al_2O_3$). This study could facilitate an analysis of the physical and chemical mechanisms of the manufacturing process based on the hydrothermal aging by determining the degree of dispersion of the catalysts loaded on a support, along with the physical and chemical changes in the DOC particles.

Fig. 5 shows a manufacturing process in which Pt and promoters are loaded on a γ-Al_2O_3 basis. Figs. 2 (a) and 3(a) show a trend that as pure Pt particles are extracted from the $H_2PtCl_6 \cdot 6H_2O$ precursor, they agglomerate in the range 20~50nm. On the other hand, as a result of impregnating and reducing $H_2PtCl_6 \cdot 6H_2O$ precursors on a γ -Al_2O_3 basis, as shown in Fig. 5 (a), they were well dispersed into small particles with the range 2~3nm. This is because Al_2O_3 has good thermal durability and enhances the dispersion force when catalysts are loaded on a support. Using an ultra

low temperature method, it was found that when catalysts are loaded on a support, they prevent entropy from increasing when the temperature approaches "absolute zero". This feature can enhance the degree of dispersion by preventing the catalyst particles from moving during a catalyst manufacturing process, and eventually improves the performance of the catalysts. Moreover, the using of Al_2O_3 as a support can reduce the costs because of the ultra-low temperature treatment; it also simplifies the manufacturing process. In addition, the Al_2O_3 support forms a barrier between the particles of promoter CZ (CeO_2+ZrO_2), thus preventing the particle growth during aging.

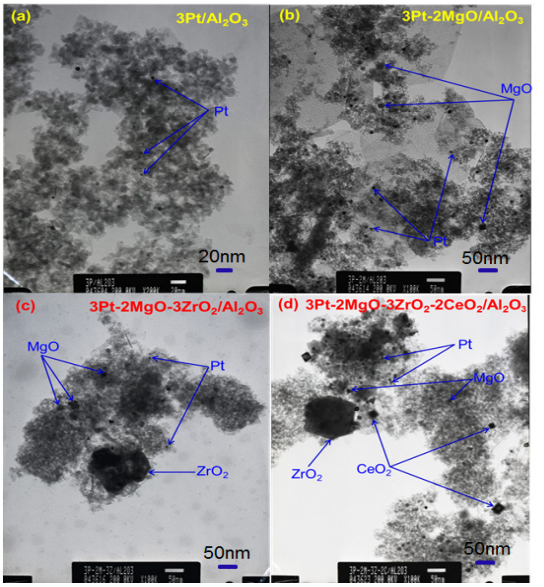

Fig. 5 TEM photographs of manufacturing process for DOC(3Pt-2MgO-3ZrO_2-2CeO_2/Al_2O_3)

Fig. 5 (b) shows a TEM photograph of 3Pt-2MgO/Al_2O_3. The particles are well dispersed in the range 10~20nm, compared with the MgO particle sizes shown in Figs. 2 (b) and 3 (b). It is believed that this phenomenon also results from the effect of the Al_2O_3 support, as previously mentioned. Fig. 5(c) shows a photographs in which 3wt% ZrO_2 is loaded for increasing the thermal durability of 3Pt-2MgO/Al_2O_3. Compared with the ZrO_2 images in Figs. 2 (c) and 3 (c), the ZrO_2 particle agglomerations are approximately 120nm class. It is determined that the agglomeration was caused by an increased thermal load because of the calcination for 6h at 500℃ when promoters are loaded. The Fig. 5 (d) shows a photograph in which 2wt% CeO_2 is loaded on a 3Pt-2MgO-3ZrO_2/Al_2O_3 basis. Compared with CeO_2 shown in Figs. 2 (d) and 3 (d), the particles are well dispersed on a the support while maintaining the same particle shape and size. The overall trend of the catalyst manufacturing process shows that when Pt, MgO and CeO_2 are loaded on a support, they are well dispersed into small particle sizes (Fig. 5).

3.3 The oxidation reaction of DOC and catalyst deactivation mechanism

The harmful gases emitted from a diesel vehicle include CO, HC, NOx, SOF and PAH. This study only considered CO, HC and NO.

$$CO+\frac{1}{2}O_2 \rightarrow CO_2 \quad (2)$$

$$C_3H_8+5O_2 \rightarrow 3CO_2+4H_2O \quad (3)$$

$$NO+\frac{1}{2}O_2 \leftrightarrow NO_2 \quad (4)$$

$$3SOF+O_2 \rightarrow CO_2+2H_2O \quad (5)$$

Equations (2)~(5) show the oxidation reaction formulae for harmful gases; the activation energies of the products differ depending on the gases. CO produces CO_2 with the least energy of 407 MJ/kmol, compared with other gases[3].

The least energy needed for a chemical reaction to progress is the activation energy, with a lower

activation energy value producing, faster reaction speed.

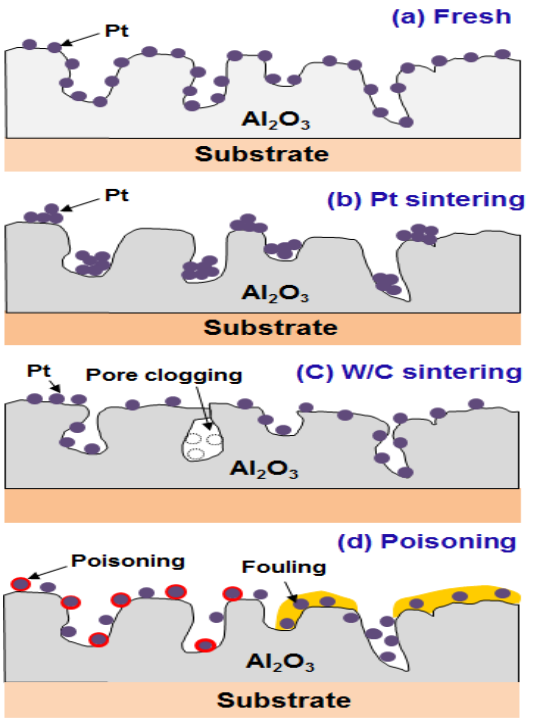

Fig. 6 Schematic of catalyst deactivation mechanism

Fig. 6 schematically shows the mechanism of the catalyst deactivation[17]. The biggest factors in catalyst deactivation are hydrothermal aging and impurity poisoning. The former deactivates the catalyst the most because vehicle catalysts are expose to a high temperature accompanied by water. Figs. 6 (b) and (c) show the schematic diagram of deactivation caused by aging. In Fig. 6 (b), Pt exposed to a high temperature sinters and agglomerates the components of the same type. Thus, aging deactivates the catalysts and the LOT (light off temperature) is gradually realized in a high-temperature region, Therfore, the reaction temperature should be raised to maintain the conversion rate.

Fig. 6 (c) shows the phenomenon of washcoat (W/C) sintering and pore clogging caused by aging. This reduces the catalyst reaction sites by reducing their specific surface area (BET). To reduce the washcoat sintering, suitable stabilizers should be optimized. Fig. 6 (d) shows that Pt is poisoned and fouled by factors such as Pb, Hg, Cd, and SO_2, which reduces the performance of catalysts by intercepting the activation points. To recover the catalyst performance, they can be activated by a heat treatment at a high temperature.

3.4 Physical and chemical characteristics based on hydrothermal aging of 3Pt-2MgO-3ZrO_2-2CeO_2/Al_2O_3 DOC

Fig. 7 shows the conversion rates for harmful gases by fresh and aged (700℃ and 800℃, 9h) catalysts of 3Pt-2MgO-3ZrO_2-2CeO_2/Al_2O_3 DOC.

For the fresh catalysts in Fig. 7 (a), CO reaches LOT 50 at a catalyst temperature of 150℃. The activation energy needed for the oxidation reaction of CO into CO_2 is low, Thus, CO is reduced by 100% at a catalyst temperature of ~225℃. when side reaction is conducted in competition reaction with CO, NO shows a maximum conversion rate of ~45% at a catalyst temperature of 300℃. The conversion rate of NO decreases as the temperature becomes above 300℃. In addition, the conversion rate of THC (C_3H_8) is lower than that of CO and NO, because its activation energy is 2110 MJ/kmol, which is five times higher than that of CO (407 MJ/kmol). Pt has a high selectivity for the oxidation reaction of CO and NOx, and Pd shows an excellent heat resistance and high selectivity with HC, Therefore, they are used to purify HC.

Fig. 7 (b) shows the conversion rate of harmful gases by a catalyst that has been hydrothermally aged catalyst for 9h at 700℃ in an air atmosphere containing 5wt% water. Because the temperature at

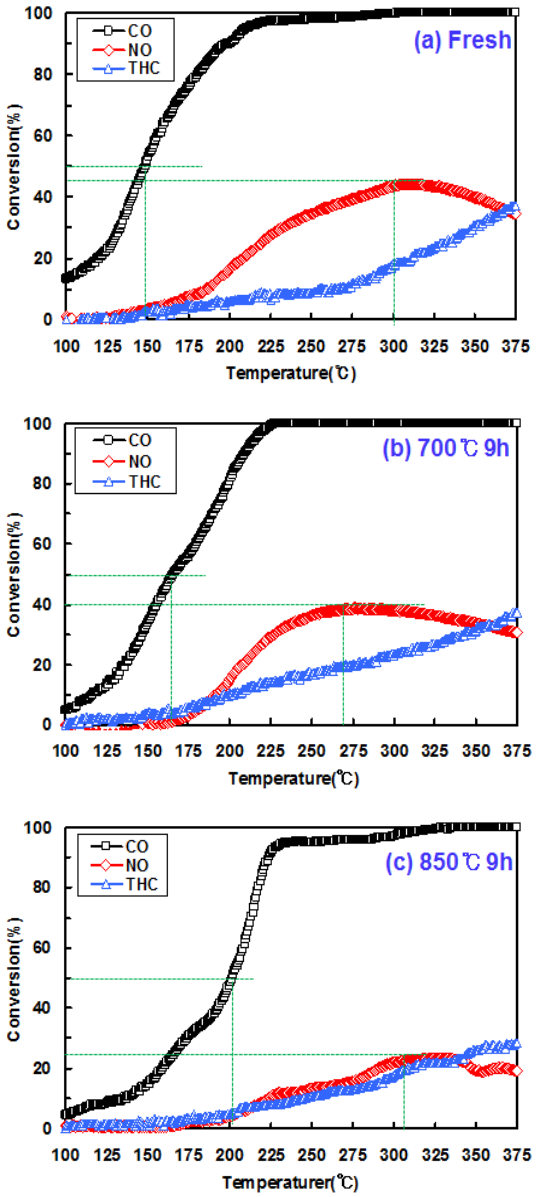

Fig. 7 The conversion rate according to hydrothermal aging of DOC

which CO approaches LOT 50 is 165℃, it was activated at temperatures higher than 15℃ compared to those of fresh catalysts and was decreased by 100% at 225℃. The conversion rate of NO reached a maximum of 40% at approximately 270℃, which was approximately 5% less than that achieved with a fresh catalyst; the conversion rate decreases as the temperature increased. On the other hand, the conversion rate of THC increased because of the good cracking of HC as the temperature increased.

Fig. 7 (c) shows a hydrothermally aged catalyst over-exposed to a high temperature of 850℃ for 9h. The LOT 50 of CO, which is easily oxidized into CO_2 because of its low activation energy, was 200℃. This was 50℃ higher than a fresh catalyst. The maximum conversion rates of NO (308℃) and THC (375℃) were 25% and 30%, which were 25% and 10% less than those for a fresh catalyst.

Fig. 8 shows the TEM photographs of a DOC catalyst after hydrothermal aging. In the fresh catalyst in Fig. 8 (a), Pt particles are well dispersed in a range of appoximately 2-3nm, while maintaining a constant interval between the Pt and the promoter.

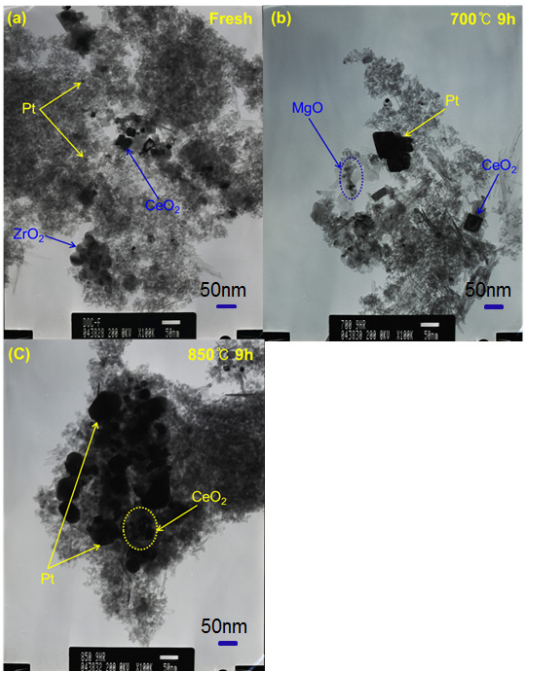

Fig. 8 TEM photographs based on the hydrothermal aging of DOC

For the hydrothermally aged catalyst for 9h at 700℃ (Fig. 8 (b)), Pt shows agglomeration among the components of the same type and grows to 70nm. Promoter CeO_2 grew to an about 50nm, which was larger than the fresh catalyst (20nm). On the other hand, the size of MgO particles increased in the pores of Al_2O_3 with an amorphous shape, agglomerating approximately 10nm.

Fig. 9 shows the specific surface area based on the hydrothermal aging. For a hydrothermally aged catalyst for 9h at 700℃, its performance in the purification of harmful gases decreased compared to a fresh catalyst as shown in Fig. 7, but its specific surface area remained constant. It is judged that the performance of a catalyst has an effect on the catalyst activation reduction of precious metal Pt sintering rather than on the washcoat sintering and pore clogging. Eventually, for the optimum performance of a catalyst, the reaction speed of the entire process of catalyst adsorption, reaction, and desorption is more important than the physical specific surface area.

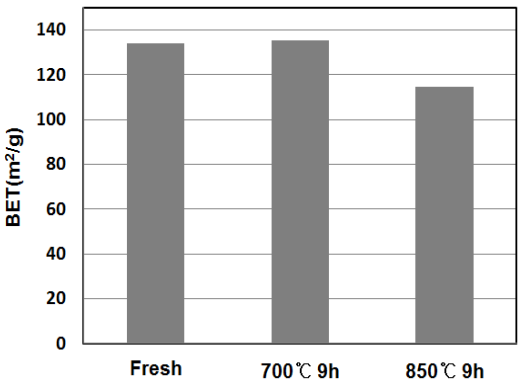

Fig. 9 BET specific surface area based on the hydrothermal aging

Fig. 8 (c) shows a catalyst that was excessively hydrothermally aged for 9h at 850℃. Pt grew to 50nm and formed a clusters, the fresh catalyst. In addition, the CeO_2 formed clusters among the components of the same type. Thus, the specific surface area was reduced to 114m^2/g, because of the sintering and agglomeration of catalyst components, which was 14% less that a fresh catalyst. Because Pt starts sintering at 700℃ and agglomerating at 850℃, an agglomerated Pt cluster causes even more deactivation of the catalysts. To avoid this problem, an appropriate combination of Pt, Rh, and Pd, which are precious metals with different features, should be optimized.

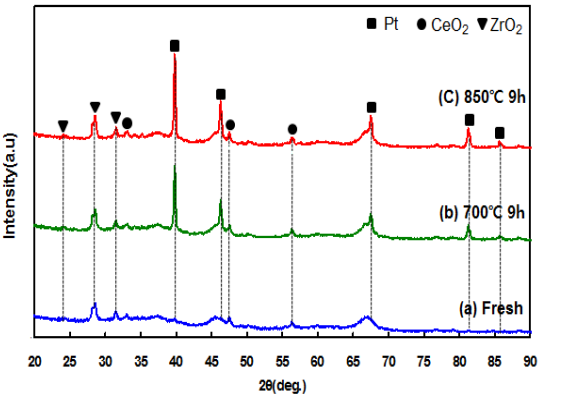

Fig. 10 XRD-spectra based on the hydrothermal aging

Fig. 10 shows the XRD-spectra based on the hydrothermal aging of the DOC catalysts. The main peak band of Pt is 2θ=39.7°; for a fresh catalyst, Pt is well dispersed into small particles, Thus, its peak intensity is not very high. However, the main peak intensity of Pt increased as the hydrothermal aging became excessive. This is because the X-ray intensity increased because of the very high agglomeration of Pt with the aging. However, any change in the crystal structure of the promoters (MgO, ZrO_2, and CeO_2) was not confirmed through from XRD peaks.

5. Conclusions

The determination of the characteristics of Pt and promoters based on the hydrothermal aging of $3Pt\text{-}2MgO\text{-}3ZrO_2\text{-}2CeO_2/Al_2O_3$ DOC catalysts led to the following conclusions.

(1) Because of the impregnation and reduction of the $H_2PtCl_6 \cdot 6H_2O$ precursors on a $\gamma\text{-}Al_2O_3$ basis, they were well dispersed into small particles with the range 2~3nm. This is because Al_2O_3 acted as a barrier that prevented the movement of catalyst particles.

(2) For a catalyst that was hydrothermally aged for 9h at 700℃, its performance in the purification of harmful gases decreased compared to that of a fresh catalyst; however, its specific surface area remained constant. This was because the performance of the catalyst was reduced by the sintering of Pt, rather than by washcoat sintering and pore clogging.

(3) For a catalyst that was excessively hydrothermally aged for 9h at 850℃, Pt grew to 50nm and formed clusters compared to a fresh catalyst. The CeO_2 promoters also formed clusters among the components of the same type, reducing their specific surface area to 114m2/g, which was 14% less than that of a fresh catalyst.

Acknowledgement

This study was supported by the academic research fund of howon university.

References

1. C. K. Seo, B. C. Choi and Y. K. Kim, 2013, “Volume Optimization of a Combined System of LNT and SCR Catalyst Considering Economic Feasibility and De-NOx Performance”, Journal of the Korea Society For Power System, Vol. 17, pp. 19-26.
2. W. S. Kang, B. C. Choi and H. N. Kim, 2013, “Characteristics of the Simultaneous Removal of PM and NOx Using CuNb-ZSM-5 Coated on Diesel Particulate Filter”, Journal of Industrial and Engineering Chemistry, Vol. 19, pp. 1406-1412.
3. J. Stepanek, P. Koci, F. Plat, M. Marek, and M. Kubicek, 2010, “Investigation of Combinded DOC and NSRC Disel Car Exhaust Catalyst” Computers and Chemical Engineering, Vol. 34, pp.744-752.
4. M. H. Wiebenga, C. H. Kim, S. J. Schmieg, S. H. Oh, D. B. Brown, D. H. Kim, J. H, Lee, C and H. F. Peden, 2012, “Deactivation Mechanism of Pt/Pd-based Oxidation Catalysts”, Vol. 184, pp. 197-204.
5. A. Winkler, D. Ferri and M. Aguirre, 2009, “The Influence of Chemical and Thermal Aging on the Catalytic Activitiy of a Monolithic Diesel Oxidation Catalyst”, Applied Catalysis B, Vol. 93, pp. 177-184.
6. S. Ye, Y. H. Yap, S. T. Kolaczkowski, k. Robinson and D. Lukyanov, “Catalyst ‘Light-off’ Experiments on a Diesel Oxidation Catalyst Connected to a Diesel Engine-Methodology and Techniques”, Chemical Engineering Research and Design Vol. 90, pp. 834-845.
7. J. E. Johnson and D. B, Kittelson, 1996, “Depostion, Diffusion and Adsorption in the Diesel Oxidation Catalyst”, Applied Catalysis B, Vol. 10, pp. 117-137.
8. S. Stadlbauer, H. Waschl, A. Schilling and L. D. R, “DOC Temperature Control for Low Temperature Operating Ranges with Post and Main Injection Actuation”, SAE 2013-01-1580.
9. B. C. Choi, C. H. Lee, H. J. Park, M. G. Park and B. S. Shin, “Durability Evaluate of Diesel Oxidation Catalysts”, KSAE 03-50054,

pp. 336-341.

10. S. J. Eaton, B. G. Bruce and T. J. Toops, “The Roles of Phosphorus and Soot on the Deactivation of Diesel Oxidation Catalyst”, SAE 2009-01-0628.
11. A. Knafl, M. Han, S. V. Bohac and D. N. Assanis, “Comparison of Diesel Oxidation Catalyst Performance of an Engine and a Gas Flow Reactor”, SAE 2007-01-0231.
12. S. R. Katare, J. E. Patterson and P. M. Laing, “Aged DOC is A Net Consumer of NO2”, SAE 2007-01-3984.
13. C. K. Seo, B. C. Choi, H. N. Kim, C. H. Lee and C. B. Lee, 2012, “Effect of ZrO_2 Addition on De-NOx Performance of Cu-ZSM-5 for SCR Catalyst”, Chemical Engineering Journal, Vol. 191, pp. 331-340.
14. C. K. Seo, H. N, Kim, B. C. Choi, M. T. Lim, C. H. Lee and C. B. Lee, 2011, “De-NOx Characteristics of a Combined System of LNT and SCR Catalysts According to Hydrothermal Aging and Sulfur Poisoning”, Catalysis Today, Vol. 164, pp. 507-514.
15. Z. Q. Tian, 2004, “Preparation of High Loading Pt Supported by Carbon by On-site Reduction”, Journal of Materials Science, Vol. 39, pp. 1507-1509.
16. K. W. Park, J. O. Choi and Y. E. Sung, 2003, “Structural, Chemical, and Electronic Properties of Pt/Ni Thin Film Electronics for Methanol Electrooxidation”, Journal Phys. Chem. B, Vol. 107, pp. 5851-5856.
17. Catalyst Fundamentals, DieselNet Technology Guide, www.dieselnet.com, 2000.11.